

Thermodynamic Functions of CeBr₃ and Congruently Melting M₃CeBr₆ Compounds (M = Rb, Cs)

L. Rycerz,[†] E. Ingier-Stocka,[†] M. Berkani,[‡] and M. Gaune-Escard^{*,§}

Chemical Metallurgy Group, Faculty of Chemistry, Wrocław University of Technology, Wybrzeże Wyspiańskiego 27, 50-370 Wrocław, Poland, Laboratoire des Procédés Catalytiques et Thermodynamique des Matériaux, Département de Génie des Procédés, Faculté des Sciences et des Sciences de l'Ingénieur, Université A. Mira de Béjaïa, 06000 Béjaïa, Algérie, and Ecole Polytechnique, Mécanique Energetique, Technopole de Chateau-Gombert, 5 rue Enrico Fermi, 13453 Marseille Cedex 13, France

The enthalpies of phase transitions and heat capacity were measured by differential scanning calorimetry for CeBr₃ as well as the Rb₃CeBr₆ and Cs₃CeBr₆ congruently melting compounds. A polynomial heat capacity dependence with respect to temperature was used to fit the experimental data. By combining these results with the entropy at 298.15 K, temperatures, and enthalpies of phase transitions, the thermodynamic functions of CeBr₃, Rb₃CeBr₆, and Cs₃CeBr₆ were calculated up to $T = 1100$ K.

Introduction

Several compounds may exist in LnX₃–MX mixtures (Ln = lanthanide, X = halide, M = alkali metal). These systems have relatively simple phase diagrams for light alkali metal halides (LiX and NaX), while those including KX, RbX, and CsX exhibit several compounds of stoichiometry M₃LnX₆, M₂LnX₅, and MLn₂X₇. The stability of these compounds depends on the nature both of the cations (lanthanide Ln, alkali M) and of the halide X.^{1–3} We have paid much attention to the M₃LnX₆ stoichiometric compounds that exist in most of the LnX₃–MX systems and have a more extended stability range than those of different stoichiometry. These congruently melting compounds were found^{4–7} to exist also in the CeBr₃–MBr systems (M = K, Rb, and Cs). The thermodynamic properties of the K₃CeBr₆ potassium compound have been characterized previously.⁵ The present work reports the thermodynamic properties (temperatures and enthalpies of phase transitions as well as the heat capacity ($C_{p,m}^0$)) of the M₃CeBr₆ compounds (M = Rb, Cs). Thermodynamic properties of cerium bromide are also presented.

Experimental

Chemicals. Cerium(III) bromide was synthesized from cerium(III) carbonate hydrate (Aldrich 99.9 %). Ce₂(CO₃)₃·xH₂O was dissolved in hot concentrated HBr acid. The solution was evaporated and CeBr₃·xH₂O was crystallized. Ammonium bromide was then added, and this wet mixture of hydrated CeBr₃ and NH₄Br was first slowly heated up to 450 K and then up to 570 K to remove the water. The resulting mixture was subsequently heated to 650 K for sublimation of NH₄Br. Finally, the salt was melted at 1100 K. Crude CeBr₃ was purified by distillation under reduced pressure (~0.1 Pa) in a quartz ampule at 1150 K. CeBr₃ prepared in this way was of a high purity: min. 99.9 %. Chemical analysis was performed by mercurimetric (bromine) and complexometric (cerium) methods. The results

were as follows: Ce, (36.91 ± 0.03) % (36.89 % theoretical); Br, (63.09 ± 0.04) % (63.11 % theoretical).

Rubidium and cesium bromides were Merck Suprapur reagents (min. 99.9 %). Prior to use, they were progressively heated to fusion under a gaseous HBr atmosphere. HBr in excess was then removed from the melt by argon bubbling.

The Rb₃CeBr₆ and Cs₃CeBr₆ stoichiometric compounds were prepared from CeBr₃ and rubidium or cesium bromides, which were weighed in the molar ratio 3:1. All mixtures were prepared in a glovebox filled with purified and water-free argon. Although only a small amount of sample was used for the differential scanning calorimetry (DSC) experiments [(300 to 500) mg], for each compound, batches of several grams were synthesized to avoid deviation from stoichiometry. Stoichiometric mixtures of bromides were melted in vacuum-sealed quartz ampoules in an electric furnace. Melts were homogenized by shaking and solidified. These samples were ground in an agate mortar in a glovebox. All chemicals were handled in an argon glovebox with a measured volume fraction of water of about $2 \cdot 10^{-6}$ and continuous gas purification by forced recirculation through external molecular sieves.

Measurements. The temperatures and enthalpies of phase transitions were measured with a Setaram DSC 121 differential scanning calorimeter.^{5,6} Samples of (300 to 500) mg were contained in quartz ampoules (about 6 mm diameter, 15 mm length) sealed under a reduced pressure of argon. The sidewalls of the ampoules were ground to fit the cells snugly into the heat flow detector. Experiments were conducted at heating and cooling rates of $5 \cdot \text{K min}^{-1}$.

The heat capacity was measured with the same Setaram DSC 121 operated in a stepwise mode. This so-called “step method” has been described^{2,3,5} previously. In the present heat capacity experiments, each 5 K heating step was followed by a 400 s isothermal delay. The heating rate was $1.5 \text{ K} \cdot \text{min}^{-1}$. All experiments were performed in the (400 to 1100) K temperature range. The mass difference of the quartz cells in any individual experiment did not exceed 1 mg (cell mass: (400 to 500) mg).

As described previously,⁵ $C_{p,m}$ data obtained on Al₂O₃ during calibration tests were found to be consistent with standard reference data (difference less than 1.5 %), except in the

* Corresponding author. Tel.: +33 491 106882. Fax: +33 491 117439. E-mail: marcelle.gaune-escard@polytech.univ-mrs.fr.

[†] Wrocław University of Technology.

[‡] Université A. Mira de Béjaïa.

[§] Ecole Polytechnique.

Table 1. Temperatures and Molar Enthalpies of Phase Transitions of CeBr₃ and Congruently Melting M₃CeBr₆ Compounds (M = Rb, Cs)

compound	T_{form} K	$\Delta_{\text{trs}}H_{\text{m}}$ kJ·mol ⁻¹	T_{trs} K	$\Delta_{\text{trs}}H_{\text{m}}$ kJ·mol ⁻¹	T_{fus} K	$\Delta_{\text{fus}}H_{\text{m}}$ kJ·mol ⁻¹
CeBr ₃	–	–	–	–	1006	51.2 ± 0.5
CeBr ₃	–	–	–	–	1005 ⁸	51.9 ⁸
Rb ₃ CeBr ₆	614	^a	696	8.0 ± 0.1	966	53.1 ± 0.3
Cs ₃ CeBr ₆	–	–	720	9.0 ± 0.3	1034	57.6 ± 0.9

^a Not determined because of metastable phase formation. Instead, an additional effect at 420 K with related enthalpy of 0.9 kJ·mol⁻¹ was observed.

temperature range (300 to 370) K, in which measured values were significantly larger. The vaporization of moisture condensed from air on the external grounded sidewalls of the ampoules used in the measurements may be given as a tentative explanation of discrepancies in this temperature range. Accordingly, the results of measurements in the temperature range (300 to 370) K were not taken into account in the polynomial fitting of the experimental data.

To establish the repeatability and uncertainty of the results, three different samples of each compound (from different batches) were used in the measurements. All these results were used in the calculation of coefficients in the equation describing the temperature dependence of the heat capacity as well as the standard deviation on $C_{\text{p,m}}^0$. The maximal deviations of individual series from mean values did not exceed ± 3 %.

Results and Discussion

Temperature and Enthalpy of Phase Transitions. The experimental temperatures and enthalpies of phase transitions are presented in Table 1 for CeBr₃, Rb₃CeBr₆, and Cs₃CeBr₆. As the results on Rb₃CeBr₆ and Cs₃CeBr₆ were obtained for the first time during this work, only those corresponding to CeBr₃ could be compared with literature data. Our experimental fusion temperature (1006 K) and fusion enthalpy (51.2 kJ·mol⁻¹) obtained by means of differential scanning calorimetry are in excellent agreement with values obtained by Dworkin and Bredig⁸ (1005 K and 51.9 kJ·mol⁻¹, respectively) obtained by drop calorimetry.

As discussed in detail previously,⁶ Rb₃CeBr₆ forms from RbBr and Rb₂CeBr₅ at 614 K, undergoes a solid–solid phase transition at 696 K, and melts congruently at 966 K. The enthalpy of the solid–solid phase transition (8.0 kJ·mol⁻¹) has a magnitude comparable to that of the solid–solid phase transition in several M₃LnX₆ compounds (M = Rb, Cs; Ln = lanthanide).^{2,3} By analogy to other M₃LnX₆ compounds (M = K, Rb), the formation of Rb₃CeBr₆ from Rb₂CeBr₅ and RbBr should be accompanied by large enthalpy changes [(45 to 55) kJ·mol⁻¹].^{2,3} Surprisingly, for pure Rb₃CeBr₆, no effect was observable on the corresponding DSC thermograms, and another small endothermic effect appeared at 420 K instead. It is very likely that Rb₃CeBr₆ does not decompose upon cooling and that a metastable phase of this compound is formed instead. Such a behavior has been addressed in the literature for many M₃LnCl₆ chloride compounds, and it has been postulated that those compounds that form at temperatures below 700 K may exist as a metastable phase at lower temperatures.⁹ A reconstructive phase transition is a special kind of solid-state reaction in which the arrangement of the ions is drastically changed in the structures surrounding this transition. Ions have to move from one site to another passing strong potential walls of other ions. The resulting “kinetic hindrance” can cause great difference

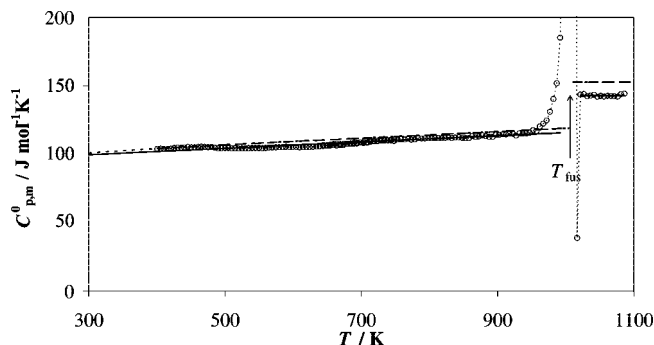


Figure 1. Molar heat capacity $C_{\text{p,m}}^0$ of CeBr₃; open circles and thin broken line, mean values from experimental results; solid lines, polynomial fitting of experimental results; thick broken lines, literature data.^{8,14}

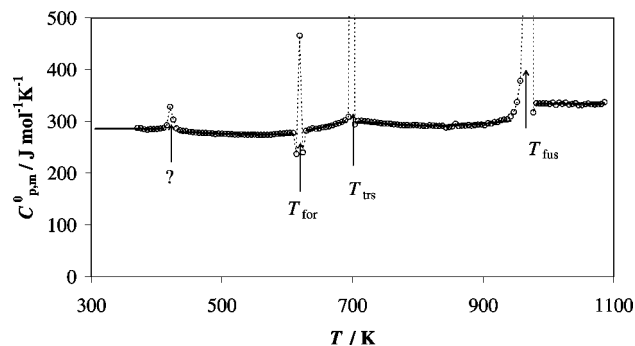


Figure 2. Molar heat capacity $C_{\text{p,m}}^0$ of Rb₃CeBr₆; open circles and broken line, mean values from experimental results; solid lines, polynomial fitting of experimental results.

between the reaction temperatures measured in DSC heating and cooling runs (thermal hysteresis).¹⁰ In extreme cases, during cooling, the “undercooling” can become so strong that the reaction does not occur in the DSC time-scale. Due to kinetic reasons, the decomposition during cooling does not occur, and the compound still exists in a metastable form. This metastability was observed for several M₃LnX₆ compounds, and no decomposition was detected during cooling runs of Rb₃PrCl₆, Rb₃NdCl₆,¹¹ K₃TbCl₆,¹² and K₃TbBr₆.¹³ Additional experiments⁶ performed on the Rb₃CeBr₆ compound, confirmed fully the compound formation at 614 K and its existence at ambient temperature as a metastable phase.

The compound with cesium, Cs₃CeBr₆, is stable or metastable at ambient temperature. It undergoes a solid–solid state transition at 720 K and melts congruently at 1034 K with the related enthalpies (9.0 and 57.6) kJ·mol⁻¹, respectively.

Heat Capacity. Experimental heat capacity data (mean values from measurements performed on three different samples) of CeBr₃, Rb₃CeBr₆, and Cs₃CeBr₆ are plotted against temperature in Figures 1 to 3. As the results on Rb₃CeBr₆ and Cs₃CeBr₆ were obtained for the first time during this work, only those corresponding to CeBr₃ could be compared with literature data.

We found that the heat capacity of solid CeBr₃ (Figure 1) varies linearly with temperature (standard deviation 1.09 J·mol⁻¹·K⁻¹). The heat capacity given by Pankratz,¹⁴ calculated from enthalpy changes measured by Dworkin and Bredig⁸ by drop calorimetry, is slightly larger in the whole temperature range (about 2 %). A constant heat capacity value, $C_{\text{p,m}}^0 = (143.00 \pm 0.74)$ J·mol⁻¹·K⁻¹, was found for liquid CeBr₃. This value is smaller by 9 % than that obtained by Dworkin and Bredig.⁸

The M₃CeBr₆ compounds (M = Rb, Cs) exhibit some specific features, rather unusual in stoichiometric binary halide com-

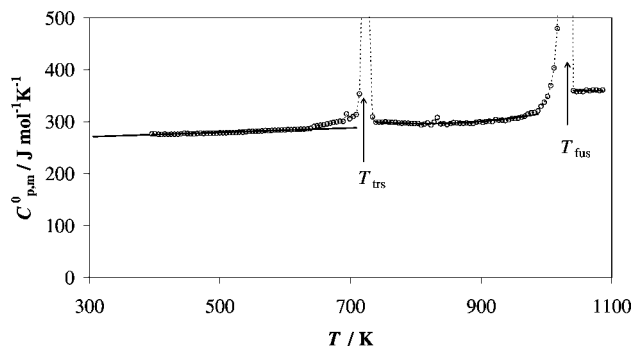


Figure 3. Molar heat capacity $C_{p,m}^0$ of Cs_3CeBr_6 : open circles and broken line, mean values from experimental results; solid lines, polynomial fitting of experimental results.

pounds, i.e., a limited temperature range of existence and a tendency for the formation of metastable phases below the decomposition temperature. These features, together with the occurrence of a solid–solid phase transition, give rise to rather complicated $C_{p,m}$ vs T plots with noticeable features related to the effects of compound formation and of phase transition, resulting in marked nonlinearity. Due to a significant rise in heat capacity, a second-order polynomial heat capacity dependence on temperature

$$C_{p,m}^0/\text{J}\cdot\text{mol}^{-1}\cdot\text{K}^{-1} = A/\text{J}\cdot\text{mol}^{-1}\cdot\text{K}^{-1} + (B/\text{J}\cdot\text{mol}^{-1}\cdot\text{K}^{-2})\cdot(T/\text{K}) + (C/\text{J}\cdot\text{mol}^{-1}\cdot\text{K}^{-3})\cdot(T/\text{K})^2 \quad (1)$$

was used to fit the experimental data. The A , B , and C coefficients in eq 1 are collected in Table 2.

The temperatures of thermal effects observed on the DSC thermograms for Rb_3CeBr_6 were confirmed by heat capacity measurements. An additional small effect at about 614 K (temperature close to that of the compound formation), not visible on DSC curves, was also detected. Accordingly, four different equations were used to account for the temperature dependence of the heat capacity for solid Rb_3CeBr_6 in the corresponding temperature ranges: (298 to 420) K, (420 to 614) K, (614 to 696) K, and (696 to 966) K with standard deviations of (5.98, 7.65, 7.28, and 8.39) $\text{J}\cdot\text{mol}^{-1}\cdot\text{K}^{-1}$, respectively. A constant heat capacity value, $C_{p,m}^0 = (333.72 \pm 9.35) \text{J}\cdot\text{mol}^{-1}\cdot\text{K}^{-1}$, was found for liquid Rb_3CeBr_6 .

Heat capacity measurements performed on Cs_3CeBr_6 evidenced two anomalies at the temperatures (720 and 1034) K, which corresponded well to the solid–solid phase transition and melting as determined from the DSC thermograms. Accordingly, experimental $C_{p,m}^0$ results of solid Cs_3CeBr_6 were fitted to a second-order polynomial dependence on temperature in the two temperature ranges, (298 to 720) K and (720 to 1034) K, with

standard deviations of (3.41 and 5.07) $\text{J}\cdot\text{mol}^{-1}\cdot\text{K}^{-1}$, respectively. As for the rubidium compound, a constant heat capacity value, $C_{p,m}^0 = (359.55 \pm 5.55) \text{J}\cdot\text{mol}^{-1}\cdot\text{K}^{-1}$, was found for liquid Cs_3CeBr_6 .

Thermodynamic Functions. For each compound, both in the solid and liquid phase, the thermodynamic functions, namely, enthalpy increments $H_m^0(T/K) - H_m^0(298.15 \text{ K})$ in $\text{J}\cdot\text{mol}^{-1}$, entropy $S_m^0(T/K)$, and Gibbs energy functions $-(G_m^0(T/K) - H_m^0(298.15 \text{ K}))/T$ in $\text{J}\cdot\text{mol}^{-1}\cdot\text{K}^{-1}$, were calculated by using the heat capacity dependence on temperature ($C_{p,m}^0/\text{J}\cdot\text{mol}^{-1}\cdot\text{K}^{-1} = f(T/K)$).

$$H_m^0(T/K) - H_m^0(298.15 \text{ K})/\text{J}\cdot\text{mol}^{-1} = (A/\text{J}\cdot\text{mol}^{-1}\cdot\text{K}^{-1})\cdot(T/K) + 1/2\cdot(B/\text{J}\cdot\text{mol}^{-1}\cdot\text{K}^{-2})\cdot(T/K)^2 + 1/3\cdot(C/\text{J}\cdot\text{mol}^{-1}\cdot\text{K}^{-3})\cdot(T/K)^3 + D/\text{J}\cdot\text{mol}^{-1} \quad (2)$$

$$S_m^0(T/K)/\text{J}\cdot\text{mol}^{-1}\cdot\text{K}^{-1} = (A/\text{J}\cdot\text{mol}^{-1}\cdot\text{K}^{-1})\ln(T/K) + (B/\text{J}\cdot\text{mol}^{-1}\cdot\text{K}^{-2})\cdot(T/K) + 1/2\cdot(C/\text{J}\cdot\text{mol}^{-1}\cdot\text{K}^{-3})\cdot(T/K)^2 + E/\text{J}\cdot\text{mol}^{-1}\cdot\text{K}^{-1} \quad (3)$$

$$-(G_m^0(T/K) - H_m^0(298.15 \text{ K}))/T = (A/\text{J}\cdot\text{mol}^{-1}\cdot\text{K}^{-1})\ln(T/K) + 1/2\cdot(B/\text{J}\cdot\text{mol}^{-1}\cdot\text{K}^{-2})\cdot(T/K) + 1/6\cdot(C/\text{J}\cdot\text{mol}^{-1}\cdot\text{K}^{-3})\cdot(T/K)^2 - (D/\text{J}\cdot\text{mol}^{-1})\cdot(T/K)^{-1} + F/\text{J}\cdot\text{mol}^{-1}\cdot\text{K}^{-1} \quad (4)$$

The parameters D , E , and F in the above equations were calculated by setting $T = 298.15 \text{ K}$ into eqs 2, 3, and 4. They are also presented in Table 2. Our experimental melting (transition) temperatures and enthalpies together with heat capacity data were used in this calculation. For both compounds, the heat capacity value $C_{p,m}^0(s, 298.15 \text{ K})$ was extrapolated from experimental results to 298.15 K (Tables 3 to 5). The value of the standard entropy at 298.15 K also necessary in these calculations was taken from the literature¹⁴ (CeBr_3) or calculated by Latimer's method from anion and cation contributions¹⁵ (Rb_3CeBr_6 and Cs_3CeBr_6). These standard entropies were (182.0, 544.3, and 570.4) $\text{J}\cdot\text{mol}^{-1}\cdot\text{K}^{-1}$ for CeBr_3 , Rb_3CeBr_6 , and Cs_3CeBr_6 , respectively. The calculated thermodynamic functions are presented in Tables 3 to 5 at selected temperatures.

From the thermodynamic data in Table 3, the enthalpy and Gibbs free energy of CeBr_3 formation ($\Delta_f H_m^0$ and $\Delta_f G_m^0$) were calculated as a function of temperature.

The formation of CeBr_3 from its elements can be described by the reaction



and the related thermodynamic functions of formation depend on the thermodynamic functions of metallic Ce and bromine Br_2 . The latter were calculated using literature data for $C_{p,m}^0$

Table 2. Thermodynamic Functions of CeBr_3 and M_3CeBr_6 Compounds ($M = \text{Rb}, \text{Cs}$): Values of A , B , C , D , E , and F Parameters in Equations 1, 2, 3, and 4

compound	T range K	A	B·10 ²	C·10 ⁴	D	E	F
		J·mol ⁻¹ ·K ⁻¹	J·mol ⁻¹ ·K ⁻²	J·mol ⁻¹ ·K ⁻³	J·mol ⁻¹	J·mol ⁻¹ ·K ⁻¹	J·mol ⁻¹ ·K ⁻¹
$\text{CeBr}_{3(s)}$	298 to 1006	92.63 ± 0.46	2.344 ± 0.06	—	-28659 ± 166	-352.76 ± 2.82	-445.39 ± 3.27
$\text{CeBr}_{3(l)}$	1006 to 1100	143.00 ± 0.74	—	—	-16268 ± 378	-628.53 ± 3.60	-769.53 ± 5.09
$\text{Rb}_3\text{CeBr}_{6(s)}$	298 to 420	264.95 ± 5.07	0.136 ± 0.021	—	-79060 ± 1520	-1082.45 ± 87.81	-1230.65 ± 34.03
$\text{Rb}_3\text{CeBr}_{6(s)}$	420 to 614	339.04 ± 6.28	-21.829 ± 1.926	1.8611 ± 0.2144	-94450 ± 820	-1287.39 ± 77.59	-1674.16 ± 34.28
$\text{Rb}_3\text{CeBr}_{6(s)}$	614 to 696	90.24 ± 7.21	30.394 ± 3.113	—	-25770 ± 9200	24.34 ± 110.42	-113.64 ± 69.37
$\text{Rb}_3\text{CeBr}_{6(s)}$	696 to 966	693.00 ± 58.49	-97.671 ± 10.283	5.9468 ± 0.6413	-193970 ± 19680	-3186.53 ± 368.40	-3897.04 ± 378.55
$\text{Rb}_3\text{CeBr}_{6(l)}$	966 to 1100	333.72 ± 9.35	—	—	-70830 ± 550	-1328.16 ± 100.08	-1679.40 ± 60.72
$\text{Cs}_3\text{CeBr}_{6(s)}$	298 to 720	255.28 ± 2.05	4.748 ± 0.392	—	-78220 ± 790	-898.24 ± 12.85	-1153.51 ± 15.09
$\text{Cs}_3\text{CeBr}_{6(s)}$	720 to 1034	835.53 ± 64.29	-130.817 ± 14.980	7.9216 ± 0.8676	-234150 ± 16230	-3932.58 ± 333.69	-4768.10 ± 398.01
$\text{Cs}_3\text{CeBr}_{6(l)}$	1034 to 1100	359.55 ± 5.55	—	—	-91820 ± 2210	-1502.22 ± 33.12	-1861.75 ± 38.71

Table 3. Thermodynamic Functions of CeBr₃ at Selected Temperatures from (298.15 to 1100) K

T K	$C_{p,m}^0(T)$ J·mol ⁻¹ ·K ⁻¹	$S_m^0(T)$ J·mol ⁻¹ ·K ⁻¹	$-(G_m^0(T) - H_m^0(298.15\text{ K}))/T$ J·mol ⁻¹ ·K ⁻¹	$H_m^0(T) - H_m^0(298.15\text{ K})$ kJ·mol ⁻¹	$\Delta_{\text{form}}H_m^0(T)$ kJ·mol ⁻¹	$\Delta_{\text{form}}G_m^0(T)$ kJ·mol ⁻¹
298.15	99.62	182.00	182.00	0.00	-891.22	-843.84
300	99.66	182.61	182.00	0.18	-891.29	-844.10
331	100.39	192.45	182.52	3.29	-892.55	-848.44
331	100.39	192.45	182.52	3.29	-936.89	-848.44
400	102.01	211.61	185.94	10.27	-935.62	-846.48
500	104.35	234.62	193.45	20.59	-933.75	-844.01
600	106.69	253.85	201.96	31.14	-931.84	-841.93
700	109.04	270.48	210.58	41.92	-929.88	-840.17
800	111.38	285.19	219.01	52.95	-927.85	-838.70
900	113.73	298.44	227.11	64.20	-925.74	-837.49
998	116.02	310.31	234.70	75.46	-923.61	-836.54
998	116.02	310.31	234.70	75.46	-926.61	-836.54
1000	116.07	310.55	234.86	75.69	-926.57	-836.43
1006	116.21	311.24	235.31	76.39	-926.44	-836.08
1006	143.00	362.13	235.31	127.59	-925.24	-836.08
1071	143.00	371.09	243.28	136.89	-872.07	-838.71
1071	143.00	371.09	243.28	136.89	-877.27	-838.71
1100	143.00	374.91	246.70	141.03	-875.85	-839.81

Table 4. Thermodynamic Functions of Rb₃CeBr₆ at Selected Temperatures from (298.15 to 1100) K

T K	$C_{p,m}^0(T)$ J·mol ⁻¹ ·K ⁻¹	$S_m^0(T)$ J·mol ⁻¹ ·K ⁻¹	$-(G_m^0(T) - H_m^0(298.15\text{ K}))/T$ J·mol ⁻¹ ·K ⁻¹	$H_m^0(T) - H_m^0(298.15\text{ K})$ kJ·mol ⁻¹
298.15	265.42	544.30	544.30	0.00
300	265.42	546.67	544.31	0.49
400	265.58	662.19	554.71	27.03
420	265.61	682.97	558.24	32.34
420	280.19	685.23	558.24	33.29
500	276.42	733.73	574.92	55.54
600	275.07	783.95	597.75	83.08
614	275.18	790.30	600.98	86.93
614	276.86	765.96	600.98	86.93
696	301.78	802.19	619.81	110.65
696	301.28	813.65	619.81	118.62
700	300.70	815.37	620.82	119.83
800	292.23	854.84	645.48	149.38
900	295.65	889.34	668.75	178.67
966	304.43	910.54	683.35	198.44
966	333.72	965.55	683.35	251.54
1000	333.72	977.10	692.55	262.89
1100	333.72	1008.90	718.29	296.26

Table 5. Thermodynamic Functions of Cs₃CeBr₆ at Selected Temperatures from (298.15 to 1100) K

T K	$C_{p,m}^0(T)$ J·mol ⁻¹ ·K ⁻¹	$S_m^0(T)$ J·mol ⁻¹ ·K ⁻¹	$-(G_m^0(T) - H_m^0(298.15\text{ K}))/T$ J·mol ⁻¹ ·K ⁻¹	$H_m^0(T) - H_m^0(298.15\text{ K})$ kJ·mol ⁻¹
298.15	269.44	570.40	570.40	0.00
300	269.52	572.07	570.41	0.50
400	274.27	650.25	581.04	27.69
500	279.02	711.97	601.27	55.36
600	283.77	763.26	624.11	83.49
700	288.52	807.36	647.21	112.11
720	289.47	815.50	651.77	117.89
720	304.30	828.03	651.77	126.91
800	295.98	859.57	671.01	150.86
900	299.83	894.50	693.94	180.51
1000	319.52	926.97	715.63	211.35
1034	329.83	937.82	722.76	222.38
1034	359.55	993.48	722.76	279.95
1100	359.55	1015.73	739.67	303.69

and $S_m^0(298.15\text{ K})$.¹⁶ The enthalpy of CeBr₃ formation at 298.15 K, $\Delta_f H_m^0(\text{CeBr}_3, \text{s}, 298.15\text{ K}) = -891.2\text{ kJ}\cdot\text{mol}^{-1}$, also required in this calculation, was taken from Cordfunke and Konings.¹⁷

Four phase changes occur in the system described by eq 5: boiling of bromine¹⁶ at 331 K with an enthalpy of 29.56 kJ·mol⁻¹, fcc→bcc solid–solid phase transition¹⁶ of Ce at 998

K with an enthalpy of 3.0 kJ·mol⁻¹, melting of CeBr₃ at 1006 K, melting¹⁶ of Ce at 1071 K with an enthalpy of 5.2 kJ·mol⁻¹. Accordingly, the formation enthalpy $\Delta_f H_m^0$ (kJ·mol⁻¹) and Gibbs energy of formation $\Delta_f G_m^0$ (kJ·mol⁻¹) of CeBr₃ are described by the equations given below:

CeBr₃ solid, 298.15 K < T < 331 K:

$$\Delta_f H_m^0/\text{kJ}\cdot\text{mol}^{-1} = (-43.345 \cdot 10^{-3}/\text{kJ}\cdot\text{mol}^{-1}\cdot\text{K}^{-1}) \cdot (T/\text{K}) + (0.41905 \cdot 10^{-6}/\text{kJ}\cdot\text{mol}^{-1}\cdot\text{K}^{-2}) \cdot (T/\text{K})^2 - 878.7/\text{kJ}\cdot\text{mol}^{-1}$$

$$\Delta_f G_m^0/\text{kJ}\cdot\text{mol}^{-1} = (-184.60 \cdot 10^{-3}/\text{kJ}\cdot\text{mol}^{-1}\cdot\text{K}^{-1}) \cdot (T/\text{K}) - (0.41905 \cdot 10^{-6}/\text{kJ}\cdot\text{mol}^{-1}\cdot\text{K}^{-2}) \cdot (T/\text{K})^2 + (6.98 \cdot 10^{-3}/\text{kJ}\cdot\text{mol}^{-1}\cdot\text{K}^{-1}) \cdot (T/\text{K}) \ln(T/\text{K}) - 800.3/\text{kJ}\cdot\text{mol}^{-1}$$

CeBr₃ solid, 331 K < T < 998 K:

$$\Delta_f H_m^0/\text{kJ}\cdot\text{mol}^{-1} = (14.21 \cdot 10^{-3}/\text{kJ}\cdot\text{mol}^{-1}\cdot\text{K}^{-1}) \cdot (T/\text{K}) + (0.38445 \cdot 10^{-5}/\text{kJ}\cdot\text{mol}^{-1}\cdot\text{K}^{-2}) \cdot (T/\text{K})^2 - (1.95 \cdot 10^2/\text{kJ}\cdot\text{mol}^{-1}\cdot\text{K}) \cdot (T/\text{K})^{-1} - 941.4/\text{kJ}\cdot\text{mol}^{-1}$$

$$\Delta_f G_m^0/\text{kJ}\cdot\text{mol}^{-1} = (129.32 \cdot 10^{-3}/\text{kJ}\cdot\text{mol}^{-1}\cdot\text{K}^{-1}) \cdot (T/\text{K}) - (0.38465 \cdot 10^{-5}/\text{kJ}\cdot\text{mol}^{-1}\cdot\text{K}^{-2}) \cdot (T/\text{K})^2 - (0.975 \cdot 10^2/\text{kJ}\cdot\text{mol}^{-1}\cdot\text{K}) \cdot (T/\text{K})^{-1} - (14.31 \cdot 10^{-3}/\text{kJ}\cdot\text{mol}^{-1}\cdot\text{K}^{-1}) \cdot (T/\text{K}) \ln(T/\text{K}) - 863.0/\text{kJ}\cdot\text{mol}^{-1}$$

CeBr₃ solid, 998 K < T < 1006 K:

$$\Delta_f H_m^0/\text{kJ}\cdot\text{mol}^{-1} = -(1.07 \cdot 10^{-3}/\text{kJ}\cdot\text{mol}^{-1}\cdot\text{K}^{-1}) \cdot (T/\text{K}) + (1.13755 \cdot 10^{-5}/\text{kJ}\cdot\text{mol}^{-1}\cdot\text{K}^{-2}) \cdot (T/\text{K})^2 - (1.95 \cdot 10^2/\text{kJ}\cdot\text{mol}^{-1}\cdot\text{K}^{-1}) \cdot (T/\text{K})^{-1} - 936.7/\text{kJ}\cdot\text{mol}^{-1}$$

$$\Delta_f G_m^0/\text{kJ}\cdot\text{mol}^{-1} = -(19.53 \cdot 10^{-3}/\text{kJ}\cdot\text{mol}^{-1}\cdot\text{K}^{-1}) \cdot (T/\text{K}) + (3.413 \cdot 10^{-5}/\text{kJ}\cdot\text{mol}^{-1}\cdot\text{K}^{-2}) \cdot (T/\text{K})^2 - (0.975 \cdot 10^2/\text{kJ}\cdot\text{mol}^{-1}\cdot\text{K}^{-1}) \cdot (T/\text{K})^{-1} + (1.07 \cdot 10^{-3}/\text{kJ}\cdot\text{mol}^{-1}\cdot\text{K}^{-1}) \cdot (T/\text{K}) \ln(T/\text{K}) - 858.3/\text{kJ}\cdot\text{mol}^{-1}$$

CeBr₃ liquid, 1006 K < T < 1071 K:

$$\Delta_f H_m^0 / \text{kJ} \cdot \text{mol}^{-1} = (49.30 \cdot 10^{-3} / \text{kJ} \cdot \text{mol}^{-1} \cdot \text{K}^{-1}) \cdot (T/\text{K}) - (0.345 \cdot 10^{-6} / \text{kJ} \cdot \text{mol}^{-1} \cdot \text{K}^{-2}) \cdot (T/\text{K})^2 - (1.95 \cdot 10^2 / \text{kJ} \cdot \text{mol}^{-1} \cdot \text{K}^1) \cdot (T/\text{K})^{-1} - 924.3 / \text{kJ} \cdot \text{mol}^{-1}$$

$$\Delta_f G_m^0 / \text{kJ} \cdot \text{mol}^{-1} = (350.36 \cdot 10^{-3} / \text{kJ} \cdot \text{mol}^{-1} \cdot \text{K}^{-1}) \cdot (T/\text{K}) + (0.345 \cdot 10^{-6} / \text{kJ} \cdot \text{mol}^{-1} \cdot \text{K}^{-2}) \cdot (T/\text{K})^2 - (0.975 \cdot 10^2 / \text{kJ} \cdot \text{mol}^{-1} \cdot \text{K}^1) \cdot (T/\text{K})^{-1} - (49.30 \cdot 10^{-3} / \text{kJ} \cdot \text{mol}^{-1} \cdot \text{K}^{-1}) \cdot (T/\text{K}) \ln(T/\text{K}) - 845.90 / \text{kJ} \cdot \text{mol}^{-1}$$

CeBr₃ liquid, 1071 K < T < 1100 K:

$$\Delta_f H_m^0 / \text{kJ} \cdot \text{mol}^{-1} = (49.30 \cdot 10^{-3} / \text{kJ} \cdot \text{mol}^{-1} \cdot \text{K}^{-1}) \cdot (T/\text{K}) - 0.345 \cdot 10^{-6} / \text{kJ} \cdot \text{mol}^{-1} \cdot \text{K}^{-2} \cdot (T/\text{K})^2 - (1.95 \cdot 10^2 / \text{kJ} \cdot \text{mol}^{-1} \cdot \text{K}^1) \cdot (T/\text{K})^{-1} - 929.5 / \text{kJ} \cdot \text{mol}^{-1}$$

$$\Delta_f G_m^0 / \text{kJ} \cdot \text{mol}^{-1} = (355.22 \cdot 10^{-3} / \text{kJ} \cdot \text{mol}^{-1} \cdot \text{K}^{-1}) \cdot (T/\text{K}) + (0.345 \cdot 10^{-6} / \text{kJ} \cdot \text{mol}^{-1} \cdot \text{K}^{-2}) \cdot (T/\text{K})^2 - (0.975 \cdot 10^2 / \text{kJ} \cdot \text{mol}^{-1} \cdot \text{K}^1) \cdot (T/\text{K})^{-1} - (49.30 \cdot 10^{-3} / \text{kJ} \cdot \text{mol}^{-1} \cdot \text{K}^{-1}) \cdot (T/\text{K}) \ln(T/\text{K}) - 851.1 / \text{kJ} \cdot \text{mol}^{-1}$$

The calculated thermodynamic functions of CeBr₃ formation are presented in Table 3 at selected temperatures.

Summary

The temperatures and enthalpies of fusion as well as the heat capacities of solid and liquid CeBr₃, Rb₃CeBr₆, and Cs₃CeBr₆ were determined. These data were used to calculate the whole set of thermodynamic functions for both the solid and liquid compounds.

Acknowledgment

L.R., E.I.-S., and M.B. wish to thank the Ecole Polytechnique de Marseille for hospitality and support during this work.

Literature Cited

- Seifert, H. J. Ternary Chlorides of the Trivalent Early Lanthanides. Phase diagrams, Crystal structures and Thermodynamic Properties. *J. Therm. Anal. Calorim.* **2002**, *7*, 789–826.
- Rycerz, L. High Temperature Characterization of LnX₃ and LnX₃-AX Solid and Liquid Systems (Ln=Lanthanide, A=Alkali, X=Halide): Thermodynamics and Electrical Conductivity; Ph.D. Thesis, Marseille, 2003.
- Rycerz, L. *Thermochemistry of lanthanide halides and compounds formed in lanthanide halide-alkali metal halide systems* (in Polish); Scientific Papers of Institute of Inorganic Chemistry and Metallurgy of Rare Elements; Series Monographs 35; Wrocław University of Technology: Wrocław, 2004.
- Rycerz, L.; Ingier-Stocka, E.; Gadzuric, S.; Gaune-Escard, M. Phase Diagram and Electrical Conductivity of the CeBr₃-KBr Binary System. *Z. Naturforsch.* **2007**, *62a*, 197–204.
- Rycerz, L.; Ingier-Stocka, E.; Berkani, M.; Gaune-Escard, M. Thermodynamic Functions of Congruently Melting Compounds Formed in CeBr₃-KBr Binary System. *J. Chem. Eng. Data* **2007**, *52*, 1209–1212.
- Rycerz, L.; Ingier-Stocka, E.; Gadzuric, S.; Gaune-Escard, M. Phase diagram and electrical conductivity of the CeBr₃-RbBr binary system. *J. Alloys Comp.* **2008**, *450*, 175–180.
- Rycerz, L.; Ingier-Stocka, E.; Gaune-Escard, M. Phase diagram and electrical conductivity of the CeBr₃-CsBr binary system, to be published.
- Dworkin, A. S.; Bredig, M. A. Enthalpy of Lanthanide Chlorides, Bromides, and Iodides from 298–1300 K: Enthalpies of Fusion and Transition. *High Temp. Sci.* **1971**, *3* (1), 81–90.
- Seifert, H. J. Retarded solid state reactions III. *J. Therm. Anal. Calorim.* **1997**, *49*, 1207–1210.
- Seifert, H. J. Ternary chlorides of the trivalent late lanthanides. *J. Thermal Anal. Calorim.* **2006**, *83*, 479–505.
- Gaune-Escard, M.; Rycerz, L.; Bogacz, A.; Szczepaniak, W. Entropies of phase transitions in the M₃LnCl₆ compounds (M=K, Rb, Cs; Ln=La, Ce, Pr, Nd) and K₂LaCl₅. *J. Alloys Comp.* **1994**, *204*, 189–192.
- Rycerz, L.; Gaune-Escard, M. Enthalpies of phase transitions and heat capacity of TbCl₃ and compounds formed in TbCl₃-MCl systems (M=K, Rb, Cs). *J. Therm. Anal. Calorim.* **2002**, *68*, 973–981.
- Rycerz, L.; Gaune-Escard, M. Thermodynamic and transport properties of K₃TbX₆ congruently melting compounds formed in TbX₃-KX binary systems (X=Cl, Br). *J. Nucl. Mater.* **2005**, *344*, 124–127.
- Pankratz, L. B. Thermodynamic Properties of Halides *U S Bur Mines, Bulletin 674*, 1984.
- Spencer, P. J. Estimation of Thermodynamic Data for Metallurgical Applications. *Thermochim. Acta* **1998**, *314*, 1–21.
- Kubaschewski, O.; Alcock, C. B.; Spencer, P. J. *Materials Thermochemistry*, 6th ed.; Pergamon Press Ltd: New York, 1993.
- Cordfunke, E. H. P.; Konings, R. J. M. The enthalpies of formation of lanthanide compounds I. LnCl₃(cr), LnBr₃(cr) and LnI₃(cr). *Thermochim. Acta* **2001**, *375*, 17–50.

Received for review November 20, 2007. Accepted March 29, 2008. Financial support by the Polish Ministry of Science and Higher Education from budget on science in 2007–2010 under the grant N N204 4098 33 is gratefully acknowledged. M.B. wishes to thank the Ministry of Higher Education and Research (MESRS) Algeria for financial support during this work.

JE700686M